ORGANOMETALLICS

Article

Cite This: *Organometallics* 2018, 37, 441−447

Anticancer Activity of Bifunctional Organometallic Ru(II) Arene Complexes Containing a 7-Hydroxycoumarin Group

Jian Zhao,[†,‡] Dingyi Zhang,[†] Wuyang Hua,[†] Wanchun Li,[†] Gang Xu,[†,‡] and Shaohua Gou*[,†,‡]

[†]Pharmaceutical Research Center and School of Chemistry and Chemical Engineering and [‡]Jiangsu Province Hi-Tech Key Laboratory for Biomedical Research, Southeast University, Nanjing 211189, China

Supporting Information

ABSTRACT: Three organometallic Ru(arene) compounds bearing 7-hydroxycoumarin have been designed and synthesized. Resulting Ru(II) complexes **2**−**4** showed potent cytotoxicity against the tested cancer cell lines, much higher than either the ligand **L1** or unfunctionalized complex **1** alone. Further study indicated complexes **2**−**4** can activate the expression of Bax, induce cytochrome *c* release from the mitochondria, and finally activate caspase-3, hinting that these compounds probably induce cell apoptosis by mitochondrial pathway. Additional molecular docking study showed that complexes **2**−**4** have the potential to bind with the MEK1, and Western blot analysis confirmed that the Ru(II) complexes can prevent the phosphorylation of MEK1 and ERK1 in HCT116 cells, which helps us to further understand the anticancer mechanisms of the newly synthesized complexes. Overall, our research suggested that the ruthenium-coumarin complexes could induce cell apoptosis via inhibition of the mitochondrial and ERK signal pathways.

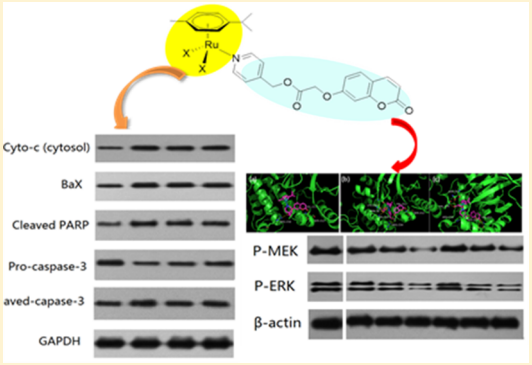

INTRODUCTION

Platinum-based anticancer drugs, such as cisplatin, carboplatin, and oxaliplatin, are well-established treatment options for a wide range of tumors, particularly in colorectal, testicular and nonsmall cell lung cancers, but they are limited by severe side effects and acquired drug resistance.[1−6] Numerous researches indicated that ruthenium-based compounds could be regarded as the promising candidates for alternative agents to take the place of platinum drugs in cancer therapy due to their lower toxicity and high selectivity.[7−14] So far, two ruthenium(III) compounds, [ImH][*trans*-Ru(DMSO)(Im)Cl_4] (NAMIA, Im = imidazole) and [IndH][*trans*-Ru(Ind)$_2Cl_4$] (KP1019, Ind = indazole), have entered clinical trials (Figure 1). However, NAMI-A failed in phase II tests, while KP1019 and its sodium salt KP1339 (sodium [trans-$RuCl_4$(1H-indazole)$_2$]) are still under clinical trials.[10,15−18] Meanwhile, organometallic Ru(II) arene complexes such as [(C_6H_5Ph)-Ru(en)Cl][PF_6] (RM175, en = ethylenediamine) and [($p^iPrC_6H_4Me$)Ru(pta)Cl_2] (RAPTA-C, pta = 1,3,5-triaza-7-phosphatricyclo[3.3.1.1]-decane) are also showing great therapeutic potential (Figure 1).[19−21] In general, arene Ru(II) complexes present a "piano stool" geometry in which arene forms the seat and the other ligands resemble the legs.[22−24] The hydrophobic arene group can influence the cellular uptake and affect the kinetic reactivity of the ruthenium(II) complex,[25,26] while the rest coordination ligands may provide more opportunities to design anticancer agents with different modes of action.[27−31]

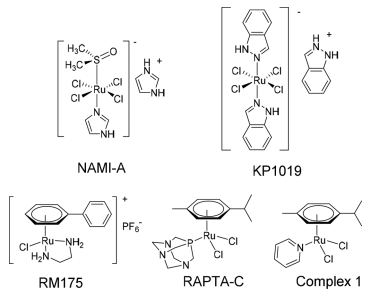

Figure 1. Related anticancer ruthenium complexes in this paper.

The ERK/MAPK (RAS/RAF/MEK/ERK) pathway plays a central role in regulating cellular growth, proliferation, and survival.[32] MEK is an intermediary in the ERK/MAPK pathway, which can be activated by RAF, leading to the subsequent phosphorylation of ERK1/2.[33] Hence, MEK has emerged as a promising molecular target for tumor therapy.[34] Coumarins, a wide class of natural compounds, showed versatile biological functions including anti-inflammatory, antioxidant, antithrombotic, and antidepressant.[35,36] Moreover, coumarin as well as its derivatives is one of the most important natural products presenting anticancer properties. Coumarins exhibited anticancer activities through various mechanisms, for example kinase inhibition, telomerase inhibition, heat shock protein (HSP90) inhibition, and cell cycle arrest.[37,38] SAR (structure−activity relationship) study revealed that the

Received: November 22, 2017
Published: January 31, 2018

DOI: 10.1021/acs.organomet.7b00842
Organometallics 2018, 37, 441−447

substitution on the coumarin ring can strongly affect the anticancer activity of the resulting compounds.[35,37] Among the diverse substitutions on the coumarin framework, O-substituted analogs of 7-hydroxycoumarins have shown desirable anticancer activities and attracted extensive interest in recent years.[35] Moreover, some studies recently revealed that 7-hydroxycoumarin derivatives can inhibit the ERK/MAPK pathway via MEK1 targeting.[33,39] These characters make coumarin a promising scaffold for anticancer agents.[40−42]

Since Ru(II) complexes have been widely studied either as single anticancer agents or in combination with other cytotoxic agents, hybridization of Ru(II) complexes and other bioactive pharmacophores is an effective strategy to design novel anticancer agents.[14] On the basis of the above study, it is rational to introduce a 7-hydroxycoumarin moiety to Ru(II) complexes to improve the pharmacological activity of the arene Ru(II) complexes. According to our assumption, the newly synthesized complexes could exhibit their anticancer activity through multiple mechanisms. Herein, a series of ruthenium−coumarin complexes were designed to evaluate the biological activities as well as the possible underlying anticancer mechanisms.

RESULTS AND DISCUSSION

Synthesis and Characterization. Ligand **L1** and complexes **2**−**4** were prepared by following the procedure shown in Scheme 1-2. 7-Hydroxycoumarin was first reacted with bromoacetic acid and then with 4-pyridinemethanol to produce ligand **L1**. Complex **2** was subsequently synthesized by treating the dimer $[Ru(\eta^6\text{-}p\text{-cymene})Cl_2]_2$ and **L1**. For complexes **3** and **4**, the dimer $[Ru(\eta^6\text{-}p\text{-cymene})Cl_2]_2$ was first treated with silver carboxylate and then with **L1** to give the target complexes. The synthesized complexes were characterized by elemental analysis, ^1H and ^{13}C NMR spectra (see Supporting Information) along with ESI-MS spectrometry. The spectral data are in good agreement with the corresponding structure of complexes **2**−**4**. Besides, the absorption and emission spectra were studied (Figure 2). Notably, complexes **2**−**4** showed similar absorption and emission spectra, but the fluorescence intensity of ligand **L1** was much higher than that of complexes **2**−**4**.

Scheme 1. Preparation of Ligand L1 and Complex 2[a]

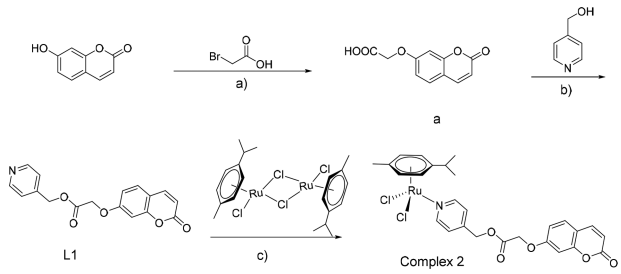

[a]Conditions: (a) K_2CO_3, KI, acetone, reflux, 8 h; (b) TBTU, Et_3N, DMF, 40 °C, 4 h; (c) CH_2Cl_2, 60 °C, 2 h.

Scheme 2. Preparation of Complexes 3 and 4[a]

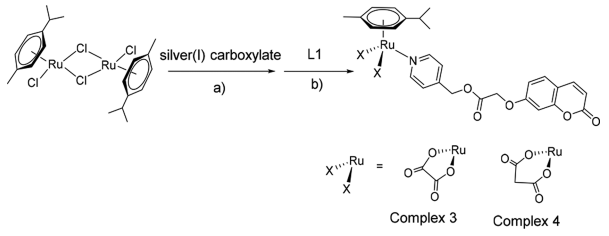

[a]Conditions: (a) H_2O, 50 °C, 24 h; (b) anhydrous methnol, 50 °C, 12 h.

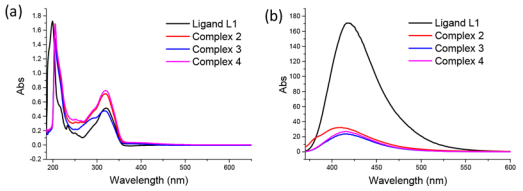

Figure 2. UV−visible absorbance (a) and emission spectra (b) of ligand **L1** and complexes **2**−**4** in H_2O/MeOH (5:95) at 25 °C.

In Vitro Cytotoxicity. The cytotoxic activities of **L1** and complexes **1**−**4** against HCT-116 (colorectal cancer), HepG-2 (hepatocellular carcinoma), and A549 (nonsmall cell lung cancer) cell lines were investigated by MTT assay with cisplatin as a positive control. The IC_{50} values (dose required to inhibit 50% cellular growth) were determined from dose-survival curves (Table 1). According to the IC_{50} values, both **L1** and complex **1** exhibited negligible cytotoxocity against the tested cell lines, while complexes **2**−**4** showed modest antiproliferative activity with the IC_{50} range from 65.6 to 161.4 μM. Obviously, the cytotoxicity of complexes **2**−**4** is much greater than either ligand **L1** or unfunctionalized complex **1** alone, indicating that both ruthenium moieties and coumarin analog played important roles in generating cytotoxic activity. However, the cytotoxicity of complexes **2**−**4** was much lower than that of cisplatin. It is worth noting that the IC_{50} values of the resulting Ru(II) arene complexes could be as low as submicromolar, but often were >100 μM such as RAPTA-C with excellent in vivo activity.[43,44] To our knowledge, the relatively hydrophobic cymene ligand of the arene Ru(II) could promote transmembrane transport, which may increase the cellular uptake of the 7-hydroxycoumarin moiety, besides these components could work synergistically toward different targets on the tumor cells. Introduction of the 7-hydroxycoumarin moiety to the Ru(II) complex is an effective way to improve the cytotoxic activity of the Ru(II) arene complex.

Table 1. In Vitro Cytotoxicity (IC_{50} μM) of Ligand L1 and Complexes 1−4 against Human Cancer Cell Lines

	IC_{50} (μM)		
compd	HCT-116[a]	HepG2[b]	A549[c]
L1	>500	>500	>500
complex **1**	460.7 ± 21.4	>500	>500
complex **2**	65.6 ± 4.6	78.7 ± 4.8	72.2 ± 6.8
complex **3**	85.07 ± 7.4	118.4 ± 9.6	86.51 ± 5.5
complex **4**	131.7 ± 7.5	143.3 ± 7.9	161.4 ± 7.5
cisplatin	15.2 ± 1.3	13.6 ± 2.8	16.5 ± 1.5

[a]Human colorectal cancer cell line. [b]Human hepatocellular carcinoma cell line. [c]Human nonsmall-cell lung cancer cell line.

Cell Cycle. The perturbation effects of ligand **L1** and complexes **1**−**4** on cell cycle progression of HCT-116 cells were analyzed by flow cytometry (Figure 3). The cell cycle data clearly showed that complexes **2**−**4** blocked the cell cycle mainly at G2/M phase with respect to the untreated control,

DOI: 10.1021/acs.organomet.7b00842
Organometallics 2018, 37, 441−447

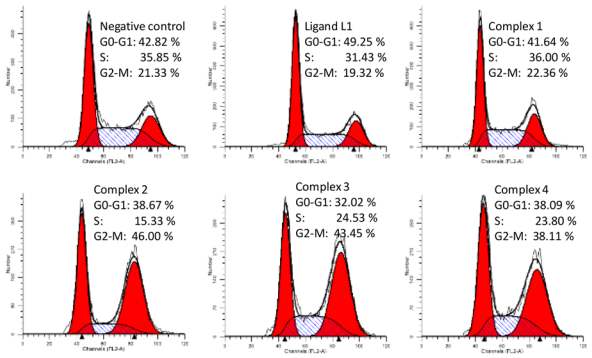

Figure 3. Cell cycle distribution upon treatment with ligand **L1** and complexes **1**−**4** in HCT-116 cells.

while free ligand **L1** induced the cell cycle at G0/G1 phase under the test conditions, indicating that there may be a little difference in the mechanisms of ligand **L1** and complexes **2**−**4**. Besides, the percentage of cancer cells arrested at the G2/M phase by complex **2** (46.00%) was higher than those of complexes **3** (43.45%) and **4** (38.11%), demonstrating that treatment with complex **2** affected the G2/M populations more than treatment with complexes **3** and **4**. However, complex **1** induced negligible changes on cell cycle distribution. This study indicated that complexes **2**−**4** arrested the cell cycle in G2/M phase in HCT-116 cells, which is similar to most of the antineoplastic drugs which induce the cell cycle in the G2/M or S phases.[45,46]

Cellular Uptake. To gain insight into the cellular behavior of the ruthenium-coumarin complexes, the intracellular uptake of complex **2** was studied by laser scanning confocal microscope (LSCM). As shown in Figure 4, complex **2** could

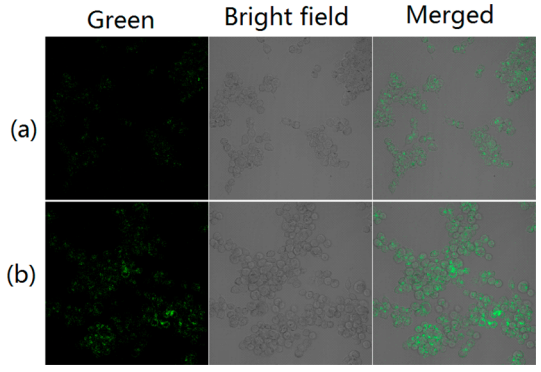

Figure 4. Confocal microscopy images of HCT-116 cells incubated with complex **2** for 3 h at 37 °C. Pictures show cells in green channel, bright-field, and the corresponding merged images: (a) complex **2** at 10 μM; (b) complex **2** at 30 μM. Cell images were obtained at an excitation wavelength of 405 nm with a (475−575 nm) emission filter.

enter into the HCT-116 cells causing intracellular fluorescence after 3 h incubation. Moreover, it was apparent that the intracellular fluorescence intensity of complex **2** at the concentration of 30 μM was higher than that of the concentration at 10 μM, indicating that the cellular uptake of complex **2** occurred in a concentration-dependent manner.

Apoptosis Study. The determination of the cellular death mechanism (necrosis or apoptosis) was performed by using an Annexin V-FITC/propidium iodide (PI) assay (Figure 5). Complexes **1**−**4** were incubated with HCT-116 cells,

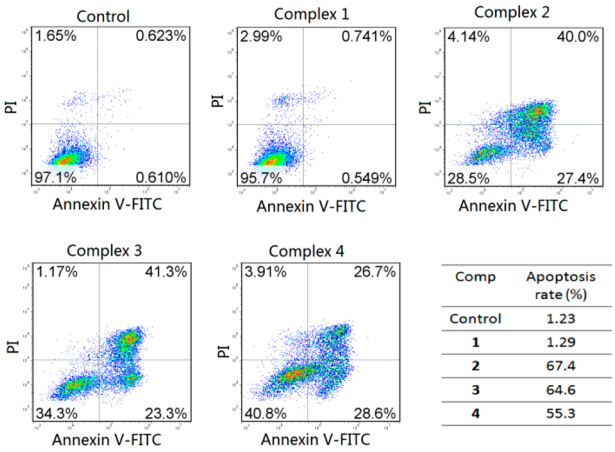

Comp	Apoptosis rate (%)
Control	1.23
1	1.29
2	67.4
3	64.6
4	55.3

Figure 5. Flow cytometry analysis for apoptosis of HCT-116 cells induced by complexes **1**−**4** at the same concentration of 150 μM for 24 h. Lower left, living cells; lower right, early apoptotic cells; upper right, late apoptotic cells; upper left, necrotic cells. Inserted numbers in the profiles indicate the percentage of the cells present in this area.

respectively, for 24 h at a concentration of 150 μM. The result is shown in Figure 5. Obviously, treatment with complexes **2**−**4** increased the early apoptotic cell populations of the HCT-116 cells compared with the negative control. The relative order of inducing apoptosis against HCT-116 cells is **2** (67.4%) > **3** (64.6%) > **4** (55.3%) > **1** (1.29%), which is consistent with the result of cytotoxicity study to some extent. Overall, complexes **2**−**4** caused cells apoptosis rather than necrosis, indicating that these three complexes produced cancer cell death through an apoptotic pathway.

To further investigate the apoptosis pathway induced by complexes **2**−**4**, Western blot assay was applied to evaluate the expression of the apoptosis-related proteins in HCT-116 cells. As shown in Figure 6, complexes **2**−**4** upregulated the

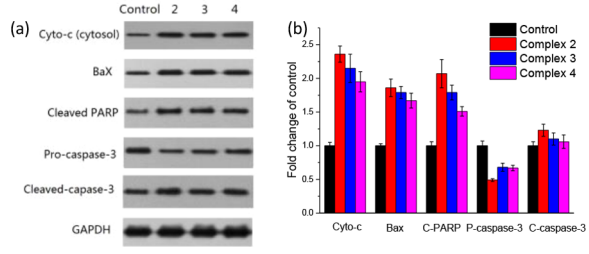

Figure 6. (a) HCT-116 cells treated with complexes **2**−**4** (20 μM) for 12 h were examined for the expression of apoptosis-regulated proteins using Western blot analysis. The data are representative of three independent experiments. (b) Densitometric analysis of the expression of apoptosis-regulated proteins normalized with GAPDH. The relative expression of each protein was represented by the density of the protein band/density of GAPDH band.

expression levels of cytochrome c (cytosol) and Bax, cleaved PARP and caspase-3, and downregulated the expression of procaspased-3, demonstrating that these complexes could activate the expression of Bax, induce cytochrome c release from the mitochondria, and finally activate caspase-3. This study indicated that complexes **2**−**4** probably induced cell apoptosis by mitochondrial pathway.

Docking Study. It was reported that coumarins can dock into the allosteric site of the MEK1 structure.[39] To further discover the anticancer mechanism of the newly synthesized

DOI: 10.1021/acs.organomet.7b00842
Organometallics 2018, 37, 441−447

ruthenium-coumarin complexes which shared the coumarin scaffold, docking study with crystal structure of MEK1 (Protein Databank (PDB) ID: 1S9J) was performed using Autodock 4.2 package.[39,47] The structures of complexes **2**–**4** were optimized at the M06-L/6-31G(d,p)//LanL2DZ level using Gaussian09 (Figure S9).[48] The docking results are shown in Figure 7.

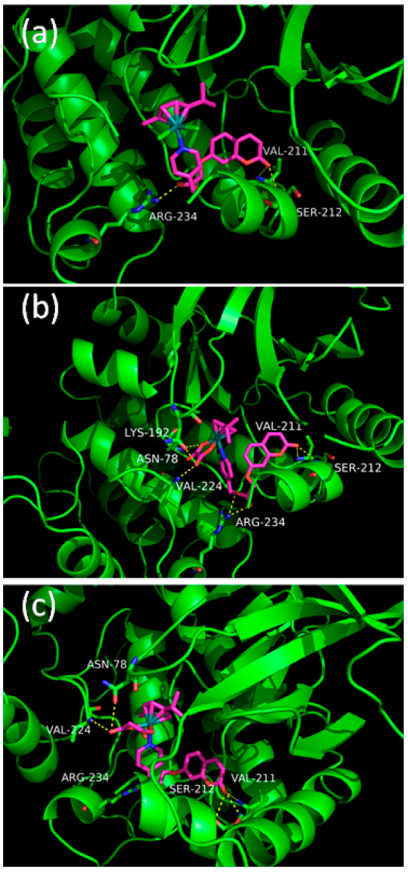

Figure 7. Binding mode of complexes **2**–**4** within the MEK1 (1S9J) allosteric catalytic site, yellow dashed lines indicate the H-bond interaction between the complex and MEK1: (a) complex **2**; (b) complex **3**; (c) complex **4**.

Obviously, for complexes **2**–**4**, the carbonyl oxygen from the coumarin ring formed two critical hydrogen bonds with residues Val211 and Ser212 in a similar manner to other published MEK1 inhibitors,[39,49] indicating that the introduction of the ruthenium moieties did not affect the binding ability of coumarin to MEK1. Moreover, the ester carbonyl group of complexes **2**–**4** also made a hydrogen bond with the backbone of Arg234. Overall, the docking experiments demonstrated that complexes **2**–**4** have the potential to bind with the MEK1.

Effects of Complexes 2 and 3 on MEK/ERK Signaling. To further determine the effect of these complexes on the ERK/MAPK pathway signaling, complexes **2** and **3** were selected to explore the effect on the protein expression of P-MEK1 and P-ERK1 in HCT116 cells. As shown in Figure 8, the expression of P-ERK1 was decreased after treatment with complexes **2** and **3**, reflecting the inhibition of the activity of MEK1. Moreover, complexes **2** and **3** also showed significant effect in suppressing MEK1 phosphorrylation, indicating that complexes **2** and **3** could also block the MEK1 being phosphorylated by upstream kinase. Thus, complexes **2** and **3** can prevent the phosphorylation of MEK1 and ERK1 in a

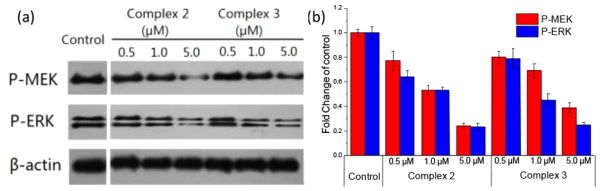

Figure 8. (a) HCT-116 cells treated with complexes **2** and **3** for 12 h were examined for the expression of P-MEK and P-ERK proteins using Western blot analysis. The data are representative of three independent experiments. (b) Densitometric analysis of the expression of P-MEK and P-ERK proteins normalized with β-actin. The relative expression of each protein was represented by the density of the protein band/density of β-actin band.

concentration-dependent manner in HCT116 cells, implying the inhibition of the downstream molecules in MAPK signal transduction.

CONCLUSION

In this study, three organometallic Ru(arene) compounds bearing 7-hydroxycoumarin pharmacophores have been synthesized and characterized. The newly synthesized ruthenium-coumarin complexes showed improved cytotoxicity against the tested cell lines, especially complex **2**, which exhibited the strongest cytotoxic activity. It was found that neither the ligand **L1** nor the unfunctionalized ruthenium analogue complex **1** showed activity on their own, indicating that the Ru(arene) compound and coumarin have a positive cooperative effect on cancer cells. Flow cytometry studies showed that complexes **2**–**4** can block the cell cycle in G2/M phase and produce death of tumor cells through an apoptotic pathway. Moreover, complexes **2**–**4** can activate the expression of Bax, induce cytochrome c release from the mitochondria, and finally activate caspase-3, hinting that these compounds probably induce cell apoptosis by mitochondrial pathway. Additional molecular docking study showed that complexes **2**–**4** have the potential to bind with the MEK1, and Western blot analysis confirmed that the resulting Ru(II) complexes can prevent the phosphorylation of MEK1 and ERK1 in HCT116 cells. All these results suggested that the newly synthesized ruthenium-coumarin complexes could induce cell apoptosis via inhibition of the mitochondrial and ERK signal pathways. Since cancer is a complicated disease, anticancer agents that act at multiple targets can improve their efficacy, which are thought to be effective way for anticancer drug design. Overall, our research indicates that the coordination of the bioactive ligand to metal fragments with established anticancer properties to obtain a synergistic effect on targeting the tumor cells may be a reasonable approach for antitumor drug development.

EXPERIMENTAL SECTION

Materials and Measurements. All chemicals and solvents were of analytical reagent grade and used without further purification. $[Ru(\eta6\text{-p-cymene})Cl_2]_2$ were prepared according to previous reports.[50] ^1H and ^{13}C NMR spectra were measured on Bruker spectrometers. Mass spectra were measured by an Agilent 6224 ESI/TOF MS instrument. Elemental analysis of C, H, and N used a Vario MICRO CHNOS elemental analyzer (Elementar). Cancer cells were obtained from Jiangsu KeyGEN BioTECH company (China). Cell cycle and apoptosis experiments were measured on a BD Accuri C6 flow cytometer and analyzed by Cell Quest software. UV−visible measurements were performed on a Shimadzu UV2600 instrument equipped with a thermostatically controlled cell holder. Fluorescence

DOI: 10.1021/acs.organomet.7b00842
Organometallics 2018, 37, 441−447

measurements were performed using a FluoroMax-4 fluorometer. Scans were run at room temperature with excitation and emission slit widths of 2.5 nm. The concentration of ligand **L1** and complexes **2**–**4** was 30 and 10 μM for absorption and emission spectra study, respectively.

Synthesis of L1. 7-Hydroxycoumarin (1.62 g, 10 mmol), potassium carbonate (6.91 g, 50 mmol), bromoacetic acid (6.95 g, 50 mmol), and acetone (250 mL) were added into a 500 mL round-bottom flask. Then a small amount of potassium iodide was added and the mixture was refluxed for 8 h. After reaction finished, water (200 mL) was added, and the pH was adjusted to ~3 by 5% HCl aqueous. Then acetone was removed under reduced pressure at room temperature, and white deposits (**a**) were obtained by filtration. Intermediate **a** (1.10 g, 5 mmol) and TBTU (1.61 g, 5 mmol) were dissolved in 100 mL of DMF, and then 4-pyridinemethanol (0.55 g, 5 mmol) and TEA (0.51 g, 5 mmol) were added and the reaction stirred at 40 °C for 4 h. The solvent was then removed by evaporation under reduced pressure. Column chromatography (eluent 15:1 DCM/methanol) gave **L1** as white solid. Yield: 0.98 g (62.8%). ESI-MS: m/z $[M + H]^+$ = 312.1. ^{1}H NMR (400 MHz, $CDCl_3$) δ 4.81 (2H, s, O=CCH_2O), 5.27 (2H, s, Py-CH_2O), 6.29–6.32 (1H, d, J = 9.2 Hz, CH=CHCO), 6.80–6.81 (1H, d, J = 2.4 Hz, OCCHC(Ar)), 6.89–6.92 (1H, d-d, J = 8.8, 2.4 Hz, OCCHCH(Ar)), 7.25–7.26 (2H, d, J = 5.6 Hz, CCH(Py)), 7.41–7.43 (1H, d, J = 8.4 Hz, OCCHCH(Ar)), 7.65–7.68 (1H, d, J = 9.2 Hz, CH=CHCO), 8.62–8.63 (2H, d, J = 6.0 Hz, NCH(Py)) ppm. ^{13}C NMR (100 MHz, DMSO-d_6) δ 65.21, 65.26, 101.75, 112.74, 113.51, 113.99, 122.12, 129.10, 143.18, 143.64, 150.20, 155.64, 160.54, 160.82, 167.63 ppm.

Synthesis of Complex 2. A solution of **L1** (0.16 g, 0.5 mmol) in dichloromethane (10 mL) was added to a suspension of $[Ru(\eta^6$-p-cymene$)Cl_2]_2$ (0.13 g, 0.21 mmol) in dichloromethane (15 mL) dropwise. The mixture was stirred at 60 °C for 2 h. Then, the reaction mixture was concentrated to 5 mL and cooling to room temperature. The crude product was separated, washed with with Et_2O (3 × 10 mL) and hexane (20 mL) (3 × 10 mL), and dried in a vacuum-dryer. Yield: 0.14 g (54.0%). Light-orange powder. Anal. Calcd (%) for $C_{27}H_{27}Cl_2NO_5Ru$: C 52.52, H 4.41, N 2.27. Found: C 52.38, H 4.58, N 2.26. ESI-MS: m/z $[M - Cl]^+$ = 582.1. ^{1}H NMR (600 MHz, $CDCl_3$) δ 1.31–1.32 (6H, d, J = 6.6 Hz, CH–(CH_3)$_2$), 2.11 (3H, s, CH_3), 2.97–3.01 (1H, m, J = 6.6 Hz, CH(CH_3)$_2$), 4.82 (2H, s, O=CCH_2O), 5.25–5.26 (2H, d, J = 4.8 Hz, CH_3CCH(Ar)), 5.27 (2H, s, Py–CH_2O), 5.46–5.47 (2H, d, J = 4.8 Hz, (CH_3)$_2$CHCCH(Ar)), 6.29–6.30 (1H, d, J = 9.6 Hz, CH=CHCO), 6.81 (1H, s, OCCHC(Ar)), 6.87–6.88 (1H, d, J = 8.4 Hz, OCCHCH(Ar)), 7.22 (2H, m, CCH(Py)), 7.42–7.44 (1H, d, J = 8.4 Hz, OCCHCH(Ar)), 7.68–7.70 (1H, d, J = 9.6 Hz, CH=CHCO), 9.01 (2H, m, NCH(Py)) ppm. ^{13}C NMR (150 MHz, DMSO-d_6) δ 18.29, 22.29, 30.70, 64.33, 65.28, 82.25, 82.81, 97.19, 101.76, 103.65, 112.76, 113.60, 113.97, 122.67, 129.34, 143.36, 146.07, 155.05, 155.64, 160.49, 160.85, 167.58 ppm.

General Procedure for Synthesis of Complexes 3 and 4. $[Ru(\eta^6$-p-cymene$)Cl_2]_2$ (0.13 g, 0.21 mmol) and silver carboxylate (0.5 mmol) were stirred in water at 50 °C for 24 h. The mixture was filtered to remove the AgCl precipitate. The solvent was removed under vacuum, and the residue was redissolved in methanol (20 mL). **L1** (0.16 g, 0.5 mmol) was added, and the mixture was stirred at 50 °C for 12 h. The solvent was reduced to 5 mL, and diethyl ether (25 mL) was added to precipitate the product. The precipitate was filtered, washed with Et_2O (3 × 10 mL) and hexane (20 mL) (3 × 10 mL), and dried in a vacuum-dryer.

Complex 3. Yield: 0.16 g (60.0%). Light-orange powder. Anal. Calcd (%) for $C_{29}H_{27}NO_9Ru$: C 54.89, H 4.29, N 2.21. Found: C 54.73, H 4.44, N 2.06. ESI-MS: m/z $[M + Na]^+$ = 658.1. ^{1}H NMR (400 MHz, $CDCl_3$) δ 1.24–1.26 (6H, d, J = 6.8 Hz, CH–(CH_3)$_2$), 2.03 (3H, s, CH_3), 2.72–2.79 (1H, m, J = 6.8 Hz, CH(CH_3)$_2$), 5.12 (2H, s, O=CCH_2O), 5.36 (2H, s, Py–CH_2O), 5.56–5.58 (2H, d, J = 6.0 Hz, CH_3CCH(Ar)), 5.80–5.82 (2H, d, J = 6.0 Hz, (CH_3)$_2$CHCCH(Ar)), 6.32–6.35 (1H, d, J = 9.2 Hz, CH=CHCO), 7.00–7.02 (1H, d, J = 8.4 Hz, OCCHCH(Ar)), 7.09 (1H, s, OCCHC(Ar)), 7.58–7.59 (2H, d, J = 6.0 Hz, CCH(Py)), 7.64–7.67 (1H, d, J = 8.4 Hz, OCCHCH(Ar)), 8.01–8.04 (1H, d, J = 9.6 Hz, CH=CHCO), 8.45–8.47 (2H, d, J = 6.0 Hz, NCH(Py)) ppm. ^{13}C NMR (75 MHz, DMSO-d_6) δ 17.68, 22.59, 30.94, 64.22, 65.32, 80.50, 83.01, 97.32, 100.91, 102.12, 113.11, 113.46, 123.86, 130.06, 144.72, 148.60, 153.26, 155.66, 160.67, 161.04, 164.78, 168.47 ppm.

Complex 4. Yield: 0.19 g (69.7%). Light-orange powder. Anal. Calcd (%) for $C_{30}H_{29}NO_9Ru$: C 55.55, H 4.51, N 2.16. Found: C 55.72, H 4.54, N 2.03. ESI-MS: m/z $[M + H]^+$ = 650.1 (50%). ^{1}H NMR (400 MHz, $CDCl_3$) δ 1.28–1.30 (6H, d, J = 6.8 Hz, CH–(CH_3)$_2$), 2.17 (3H, s, CH_3), 2.76–2.85 (1H, m, overlapped, J = 6.8 Hz, CH(CH_3)$_2$), 2.82–2.86 (1H, d, J = 15.6 Hz, OOCCH_2COO), 3.43–3.47 (1H, d, J = 15.6 Hz, OOCCH_2COO), 4.85 (2H, s, O=CCH_2O), 5.28 (2H, s, Py–CH_2O), 5.35–5.37 (2H, d, J = 6.0 Hz, CH_3CCH(Ar)), 5.50–5.52 (2H, d, J = 6.0 Hz, (CH_3)$_2$CHCCH(Ar)), 6.28–6.31 (1H, d, J = 9.2 Hz, CH=CHCO), 6.80 (1H, s, OCCHC(Ar)), 6.89–6.91 (1H, d, J = 8.4 Hz, OCCHCH(Ar)), 7.28–7.29 (2H, d, J = 6.0 Hz, CCH(Py)), 7.43–7.45 (1H, d, J = 8.4 Hz, OCCHCH(Ar)), 7.69–7.72 (1H, d, J = 9.6 Hz, CH=CHCO), 8.66–8.68 (2H, d, J = 6.4 Hz, NCH(Py)) ppm. ^{13}C NMR (100 MHz, DMSO-d_6) δ 17.88, 22.37, 30.66, 46.73, 64.07, 65.17, 81.42, 82.00, 97.27, 101.69, 102.58, 112.86, 113.57, 113.87, 123.40, 129.34, 143.48, 147.20, 152.89, 155.58, 160.50, 160.94, 167.64, 174.56 ppm.

Docking Studies. Docking studies were carried out using Autodock Dock 4.2. The crystal data of MEK1 was obtained from the Protein Databank (PDB ID: 1S9J). Small molecules in 1S9J were removed prior to the docking by software PyMOL. The docking simulation was performed with the Lamarckian genetic algorithm for as much as 150 docking runs. Each run of the docking operation was terminated after a maximum of 2 500 000 energy evaluations. During docking studies, the protein structure was kept rigid. Rotation in complexes **2**–**4** was permitted about all single bonds.

Cell Culture. Three human tumor cell lines, HCT-116 (human colorectal cancer), HepG2 (human hepatocellular carcinoma), and A549 (human non-small-cell lung cancer) were maintained in a humidified atmosphere of 5% CO_2 and 95% air at 37 °C. They were cultured in RPMI-1640 medium supplemented with 10% fetal bovine serum (FBS), 100 μg/mL penicillin, and 100 μg/mL streptomycin.

MTT Assay. The IC_{50} values of all compounds were determined by means of the colorimetric assay MTT assay. This assay is based on the cleavage of the yellow tetrazolium salt (3-(4,5-dimethylthiazol-2-yl)-2,5-diphenyl tetrazolium bromide; MTT, Sigma), forming purple formazan crystals by viable cells. The cultured cells were plated in 96-well culture plates at a density of 5000 cells per well and incubated for 24 h at 37 °C in a 5% CO_2 incubator. The compounds were dissolved in DMF and then diluted to the required concentration with culture medium (the final concentration of DMF was less than 0.4%). The diluted complexes were then added to the wells, and cells were incubated at 37 °C for 72 h. Afterward, the cells were treated with 20 μL MTT dye solution (5 mg/mL) for 4 h cultivation. The media with MTT were removed and replaced with DMSO (150 μL). The UV absorption intensity was detected with an ELISA reader at 490 nm. The IC_{50} values were calculated by SPSS software after three parallel experiments.

Cell Cycle Measurement. HCT-116 cells were transferred into 6-well plates and cultured overnight at 37 °C. Then, ligand **L1** (30 μM) and complexes **1**–**4** (30 μM) were incubated with cells for 24 h. All adherent and floating cells were collected and washed with PBS and fixed with 70% ethanol at 4 °C for 24 h. After being centrifuged, cells were stained with 50 μg/mL propidium iodide solution containing 100 μg/mL RNase for 0.5 h at 37 °C. The samples were measured by flow cytometry (FAC Scan, Becton Dickenson) using Cell Quest software and recording propidium iodide (PI) in the FL2 channel.

Cellular Uptake. HCT116 cells were cultured in a 6-well plate containing a coverslip. Then the cells were incubated with complex **1** at the concentrations of 10 and 30 μM for 3 h. After that, the cells were washed with PBS for three times to wipe out the free drug. Then, the coverslip was taken out and put on a glass slid. The glass slid was detected by LSCM operating at a 405 nm excitation wavelength.

Apoptosis Study. Specific operations were as follows: After induced apoptosis of HCT-116 cells by the addition of ligand **L1** (30

DOI: 10.1021/acs.organomet.7b00842
Organometallics 2018, 37, 441–447

μM) and complexes **1**−**4** (30 μM) for 24 h, cells were digested with trypsin and washed twice with cold PBS and collected by centrifugation (5 min, 25 °C, 2000 rpm). After that, cells were resuspended in binding buffer (10 mM Hepes, 140 mM NaCl, 2.5 mM $CaCl_2$, pH 7.4) and incubated with annexin V-FITC (100 ng/mL) and then with propidium iodide (2 μg/mL) for 15 min at room temperature. The fluorescence was measured by an annexin V-FITC apoptosis detection kit (Roche) according to the manufacturer's protocol, and cells were analyzed by a computer station running Cell Quest software.

Western Blot Analysis. HCT-116 cells were cultured until the cell density reached 80%. Then, the compounds with ideal concentrations were added, and the cells were cultured for 12 h at 37 °C. Proteins were extracted by lysis buffer. The concentration of protein was measured by the BCA (bicinchoninic acid) protein assay with a Varioskan multimode microplate spectrophotometer (Thermo, Waltham, MA). Equivalent samples (20 mg/lane) were separated by 8−12% sodium dodecyl sulfate-polyacrylamide gel electrophoresis (SDS-PAGE) and transferred onto polyvinylidene difluoride (PVDF) Immobilon-P membrane (Bio-Rad) with a transblot apparatus (Bio-Rad). The blots were blocked with 5% nonfat milk in TBST (Tris-buffered saline plus 0.1% Tween 20) for 1 h, and then the membranes were incubated with the indicated primary antibodies at 4 °C overnight. After that, the membrane was washed with PBST three times and subsequently probed by the appropriate secondary antibodies conjugated to horseradish peroxidase for 1 h. Detection was performed via Odyssey scanning system (Li-COR, Lincoln, Nebraska). GAPDH or β-actin was used as loading control.

■ ASSOCIATED CONTENT

Supporting Information

The Supporting Information is available free of charge on the ACS Publications website at DOI: 10.1021/acs.organomet.7b00842.

NMR spectra and DFT-optimized structures of complexes **2**−**4** (PDF)

■ AUTHOR INFORMATION

Corresponding Author

*E-mail: sgou@seu.edu.cn.

ORCID

Shaohua Gou: 0000-0003-0284-5480

Notes

The authors declare no competing financial interest.

■ ACKNOWLEDGMENTS

We are grateful to the National Natural Science Foundation of China (Grant No. 21601034) and Jiangsu Province Natural Science Foundation (Grant No. BK20160664) for financial aid to this work. We also thank the Fundamental Research Funds for the Central Universities (Project 2242016K30020) for supplying basic facilities to our key laboratory. We also express our gratitude to the Priority Academic Program Development of Jiangsu Higher Education Institutions for the construction of fundamental facilities (Project 1107047002).

■ REFERENCES

(1) Johnstone, T. C.; Suntharalingam, K.; Lippard, S. J. *Chem. Rev.* **2016**, *116*, 3436−3486.
(2) Wheate, N. J.; Walker, S.; Craig, G. E.; Oun, R. *Dalton Trans.* **2010**, *39*, 8113−8127.
(3) Kelland, L. *Nat. Rev. Cancer* **2007**, *7*, 573−584.
(4) Galanski, M.; Keppler, B. K. *Anti-Cancer Agents Med. Chem.* **2007**, *7*, 55−73.
(5) Zhao, J.; Wang, D.; Xu, G.; Gou, S. *J. Inorg. Biochem.* **2017**, *175*, 20−28.
(6) Hambley, T. W. *Science* **2007**, *318*, 1392−1393.
(7) Yan, Y. K.; Melchart, M.; Habtemariam, A.; Sadler, P. J. *Chem. Commun.* **2005**, 4764−4776.
(8) Alessio, E.; Mestroni, G.; Bergamo, A.; Sava, G. *Curr. Top. Med. Chem.* **2004**, *4*, 1525−1535.
(9) Clarke, M. J. *Coord. Chem. Rev.* **2003**, *236*, 209−233.
(10) Trondl, R.; Heffeter, P.; Kowol, C. R.; Jakupec, M. A.; Berger, W.; Keppler, B. K. *Chem. Sci.* **2014**, *5*, 2925−2932.
(11) Hartinger, C. G.; Zorbas-Seifried, S.; Jakupec, M. A.; Kynast, B.; Zorbas, H.; Keppler, B. K. *J. Inorg. Biochem.* **2006**, *100*, 891−904.
(12) Han Ang, W.; Dyson, P. J. *Eur. J. Inorg. Chem.* **2006**, *2006*, 4003−4018.
(13) Mu, C.; Chang, S. W.; Prosser, K. E.; Leung, A. W.; Santacruz, S.; Jang, T.; Thompson, J. R.; Yapp, D. T.; Warren, J. J.; Bally, M. B.; et al. *Inorg. Chem.* **2016**, *55*, 177−190.
(14) Zeng, L.; Gupta, P.; Chen, Y.; Wang, E.; Ji, L.; Chao, H.; Chen, Z.-S. *Chem. Soc. Rev.* **2017**, *46*, 5771−5804.
(15) Hartinger, C. G.; Jakupec, M. A.; Zorbas-Seifried, S.; Groessl, M.; Egger, A.; Berger, W.; Zorbas, H.; Dyson, P. J.; Keppler, B. K. *Chem. Biodiversity* **2008**, *5*, 2140−2155.
(16) Bergamo, A.; Sava, G. *Dalton Trans.* **2011**, *40*, 7817−7823.
(17) Sadafi, F.; Massai, L.; Bartolommei, G.; Moncelli, M. R.; Messori, L.; Tadini-Buoninsegni, F. *ChemMedChem* **2014**, *9*, 1660−1664.
(18) Sava, G.; Zorzet, S.; Turrin, C.; Vita, F.; Soranzo, M.; Zabucchi, G.; Cocchietto, M.; Bergamo, A.; DiGiovine, S.; Pezzoni, G. *Clin. Cancer Res.* **2003**, *9*, 1898−1905.
(19) Guichard, S.; Else, R.; Reid, E.; Zeitlin, B.; Aird, R.; Muir, M.; Dodds, M.; Fiebig, H.; Sadler, P.; Jodrell, D. *Biochem. Pharmacol.* **2006**, *71*, 408−415.
(20) Scolaro, C.; Bergamo, A.; Brescacin, L.; Delfino, R.; Cocchietto, M.; Laurenczy, G.; Geldbach, T. J.; Sava, G.; Dyson, P. J. *J. Med. Chem.* **2005**, *48*, 4161−4171.
(21) Renfrew, A. K.; Phillips, A. D.; Tapavicza, E.; Scopelliti, R.; Rothlisberger, U.; Dyson, P. J. *Organometallics* **2009**, *28*, 5061−5071.
(22) Smith, G. S.; Therrien, B. *Dalton Trans* **2011**, *40*, 10793−10800.
(23) Zhang, Y.; Zheng, W.; Luo, Q.; Zhao, Y.; Zhang, E.; Liu, S.; Wang, F. *Dalton Trans* **2015**, *44*, 13100−13111.
(24) Pettinari, R.; Marchetti, F.; Petrini, A.; Pettinari, C.; Lupidi, G.; Smolenski, P.; Scopelliti, R.; Riedel, T.; Dyson, P. J. *Organometallics* **2016**, *35*, 3734−3742.
(25) Wang, F.; Chen, H.; Parsons, S.; Oswald, I. D.; Davidson, J. E.; Sadler, P. J. *Chem. - Eur. J.* **2003**, *9*, 5810−5820.
(26) Wang, F.; Habtemariam, A.; van der Geer, E. P.; Fernandez, R.; Melchart, M.; Deeth, R. J.; Aird, R.; Guichard, S.; Fabbiani, F. P.; Lozano-Casal, P.; et al. *Proc. Natl. Acad. Sci. U. S. A.* **2005**, *102*, 18269−18274.
(27) Paunescu, E.; McArthur, S.; Soudani, M.; Scopelliti, R.; Dyson, P. J. *Inorg. Chem.* **2016**, *55*, 1788−1808.
(28) Bonfili, L.; Pettinari, R.; Cuccioloni, M.; Cecarini, V.; Mozzicafreddo, M.; Angeletti, M.; Lupidi, G.; Marchetti, F.; Pettinari, C.; Eleuteri, A. M. *ChemMedChem* **2012**, *7*, 2010−2020.
(29) Riedl, C. A.; Flocke, L. S.; Hejl, M.; Roller, A.; Klose, M. H.; Jakupec, M. A.; Kandioller, W.; Keppler, B. K. *Inorg. Chem.* **2017**, *56*, 528−541.
(30) Caruso, F.; Pettinari, R.; Rossi, M.; Monti, E.; Gariboldi, M. B.; Marchetti, F.; Pettinari, C.; Caruso, A.; Ramani, M. V.; Subbaraju, G. V. *J. Inorg. Biochem.* **2016**, *162*, 44−51.
(31) Ashraf, A.; Hanif, M.; Kubanik, M.; Sohnel, T.; Jamieson, S. M.; Bhattacharyya, A.; Hartinger, C. G. *J. Organomet. Chem.* **2017**, *839*, 31−37.
(32) Roberts, P. J.; Der, C. J. *Oncogene* **2007**, *26*, 3291−3310.
(33) Liu, M.-M.; Chen, X.-Y.; Huang, Y.-Q.; Feng, P.; Guo, Y.-L.; Yang, G.; Chen, Y. *J. Med. Chem.* **2014**, *57*, 9343−9356.
(34) Neuzillet, C.; Tijeras-Raballand, A.; De Mestier, L.; Cros, J.; Faivre, S.; Raymond, E. *Pharmacol. Ther.* **2014**, *141*, 160−171.

DOI: 10.1021/acs.organomet.7b00842
Organometallics 2018, 37, 441−447

(35) Emami, S.; Dadashpour, S. *Eur. J. Med. Chem.* **2015**, *102*, 611−630.
(36) Elshemy, H. A.; Zaki, M. A. *Bioorg. Med. Chem.* **2017**, *25*, 1066−1075.
(37) Thakur, A.; Singla, R.; Jaitak, V. *Eur. J. Med. Chem.* **2015**, *101*, 476−495.
(38) Skoczynska, A.; Lux, K.; Mayer, P.; Lorenz, I.-P.; Krajewska, U.; Rozalski, M.; Dolega, A.; Budzisz, E. *Inorg. Chim. Acta* **2017**, *456*, 105−112.
(39) Han, S.; Zhou, V.; Pan, S.; Liu, Y.; Hornsby, M.; McMullan, D.; Klock, H. E.; Haugen, J.; Lesley, S. A.; Gray, N.; et al. *Bioorg. Med. Chem. Lett.* **2005**, *15*, 5467−5473.
(40) Dondaine, L.; Escudero, D.; Ali, M.; Richard, P.; Denat, F.; Bettaieb, A.; Le Gendre, P.; Paul, C.; Jacquemin, D.; Goze, C.; et al. *Eur. J. Inorg. Chem.* **2016**, *2016*, 545−553.
(41) Thota, S.; Vallala, S.; Yerra, R.; Rodrigues, D. A.; Barreiro, E. J. *Med. Chem. Res.* **2016**, *25*, 2127−2132.
(42) Touisni, N.; Maresca, A.; McDonald, P. C.; Lou, Y.; Scozzafava, A.; Dedhar, S.; Winum, J.-Y.; Supuran, C. T. *J. Med. Chem.* **2011**, *54*, 8271−8277.
(43) Ang, W. H.; Daldini, E.; Scolaro, C.; Scopelliti, R.; Juillerat-Jeannerat, L.; Dyson, P. J. *Inorg. Chem.* **2006**, *45*, 9006−9013.
(44) Dyson, P. J.; Sava, G. *Dalton Trans.* **2006**, 1929−1933.
(45) Zhao, J.; Hua, W.; Xu, G.; Gou, S. *J. Inorg. Biochem.* **2017**, *176*, 175−180.
(46) Gumus, F.; Eren, G.; Acik, L.; Celebi, A.; Ozturk, F.; Yilmaz, S.; Sagkan, R. I.; Gur, S.; Ozkul, A.; Elmalı, A.; et al. *J. Med. Chem.* **2009**, *52*, 1345−1357.
(47) Morris, G. M.; Huey, R.; Lindstrom, W.; Sanner, M. F.; Belew, R. K.; Goodsell, D. S.; Olson, A. J. *J. Comput. Chem.* **2009**, *30*, 2785−2791.
(48) Frisch, M. J.; Trucks, G. W.; Schlegel, H. B.; Scuseria, G. E.; Robb, M. A.; Cheeseman, J. R.; Scalmani, G.; Barone, V.; Mennucci, B.; Petersson, G. A.; Nakatsuji, H.; Caricato, M.; Li, X.; Hratchian, H. P.; Izmaylov, A. F.; Bloino, J.; Zheng, G.; Sonnenberg, J. L.; Hada, M.; Ehara, M.; Toyota, K.; Fukuda, R.; Hasegawa, J.; Ishida, M.; Nakajima, T.; Honda, Y.; Kitao, O.; Nakai, H.; Vreven, T.; Montgomery, J. A., Jr.; Peralta, J. E.; Ogliaro, F.; Bearpark, M.; Heyd, J. J.; Brothers, E.; Kudin, K. N.; Staroverov, V. N.; Kobayashi, R.; Normand, J.; Raghavachari, K.; Rendell, A.; Burant, J. C.; Iyengar, S. S.; Tomasi, J.; Cossi, M.; Rega, N.; Millam, J. M.; Klene, M.; Knox, J. E.; Cross, J. B.; Bakken, V.; Adamo, C.; Jaramillo, J.; Gomperts, R.; Stratmann, R. E.; Yazyev, O.; Austin, A. J.; Cammi, R.; Pomelli, C.; Ochterski, J. W.; Martin, R. L.; Morokuma, K.; Zakrzewski, V. G.; Voth, G. A.; Salvador, P.; Dannenberg, J. J.; Dapprich, S.; Daniels, A. D.; Farkas, O.; Foresman, J. B.; Ortiz, J. V.; Cioslowski, J.; Fox, D. J. *Gaussian 09*, revision E.01; Gaussian, Inc.: Wallingford, CT, 2009.
(49) Sun, J.; Niu, Y.; Wang, C.; Zhang, H.; Xie, B.; Xu, F.; Jin, H.; Peng, Y.; Liang, L.; Xu, P. *Bioorg. Med. Chem.* **2016**, *24*, 3472−3482.
(50) Bennett, M. A.; Smith, A. K. *J. Chem. Soc., Dalton Trans.* **1974**, 233−241.

DOI: 10.1021/acs.organomet.7b00842
Organometallics 2018, 37, 441−447